


Amyloid-beta Hot Paper

How to cite:

doi.org/10.1002/anie.202217791

Chasing the Elusive “In-Between” State of the Copper-Amyloid β Complex by X-ray Absorption through Partial Thermal Relaxation after Photoreduction

Enrico Falcone, Germano Nobili, Michael Okafor, Olivier Proux, Giancarlo Rossi, Silvia Morante, Peter Faller,* and Francesco Stellato*

Abstract: The redox activity of Cu ions bound to the amyloid- β (A β) peptide is implicated as a source of oxidative stress in the context of Alzheimer’s disease. In order to explain the efficient redox cycling between Cu^{II}-A β (distorted square-pyramidal) and Cu^I-A β (digonal) resting states, the existence of a low-populated “in-between” state, prone to bind Cu in both oxidation states, has been postulated. Here, we exploited the partial X-ray induced photoreduction at 10 K, followed by a thermal relaxation at 200 K, to trap and characterize by X-ray Absorption Spectroscopy (XAS) a partially reduced Cu-A β ₁₋₁₆ species different from the resting states. Remarkably, the XAS spectrum is well-fitted by a previously proposed model of the “in-between” state, hence providing the first direct spectroscopic characterization of an intermediate state. The present approach could be used to explore and identify the catalytic intermediates of other relevant metal complexes.

Copper (Cu) ions are essential trace elements in most living organisms. They are present almost exclusively in two ionic forms, Cu^I or Cu^{II}, normally found in complex with proteins where they act as catalytic centers. Cu levels are tightly regulated by binding to dedicated proteins that modulate

trafficking, cellular import and export, and incorporation into appropriate enzymes. The regulation mechanism must be quite efficient, because both deficiency or overload of Cu are dangerous, as well documented in the two genetic, Menkes (Cu deficiency) and Wilson (Cu overload), diseases respectively.^[1,2]

Indeed, like a lack of Cu impairs the essential function of Cu-enzymes (e.g. cytochrome C oxidase), an excessive Cu concentration can lead to the displacement of Fe from iron-sulfur cluster proteins,^[3,4] the catalytic production of reactive oxygen species (ROS), unwanted interactions with essential cysteine residues,^[1,2,5] and induction of protein aggregation.^[6]

Cu deregulation has been reported in several neurodegenerative diseases. Misplaced Cu is supposed to bind to amyloid- β (A β) peptides in Alzheimer’s (AD)^[7] or α -synuclein in Parkinson’s (PD)^[8,9] diseases. Both peptides/proteins belong to the class of the so-called intrinsically disordered proteins (IDPs) and are prone to form amyloids, i.e. beta-sheet rich aggregates. Moreover, these Cu-peptide/protein complexes have been shown to catalyze efficiently in vitro the ROS production in the presence of dioxygen and ascorbate (a physiological reducing agent). Hence Cu-bound amyloid peptides became the target of a therapeutic approach aimed at inhibiting the over-production of Cu-induced ROS that might lead to the oxidative stress observed in AD and PD.^[10,11]

Cu complexes can produce ROS via cycling between the two redox states Cu^I and Cu^{II} in the presence of O₂. An important point to take into account is that the coordination chemistry of Cu^{II} and Cu^I are remarkably different. Differences are quite evident when Cu ions are bound to flexible peptides or IDPs.^[12,13] Indeed, flexible peptide chains can more easily adopt the local peptide structures around the

[*] E. Falcone, M. Okafor, P. Faller
 Institut de Chimie (UMR 7177),
 University of Strasbourg, CNRS
 4 Rue Blaise Pascal, 67081 Strasbourg (France)
 E-mail: pfaller@unistra.fr

G. Nobili, G. Rossi, S. Morante, F. Stellato
 Università di Roma Tor Vergata,
 Via della Ricerca Scientifica
 00133 Roma (Italy)
 and
 INFN, Sezione di Roma Tor Vergata,
 Via della Ricerca Scientifica
 00133 Roma (Italy)
 E-mail: stellato@roma2.infn.it

O. Proux
 Observatoire des Sciences de l’Univers de Grenoble,
 UMS 832 CNRS-Université Grenoble Alpes
 38041 Grenoble (France)

G. Rossi
 Centro Fermi, Museo Storico della Fisica e Centro
 Studi e Ricerche Enrico Fermi
 Via Panisperna 89a, 00184 Roma (Italy)

P. Faller
 Institut Universitaire de France (IUF)
 1 rue Descartes, 75231 Paris (France)

© 2023 The Authors. Angewandte Chemie International Edition published by Wiley-VCH GmbH. This is an open access article under the terms of the Creative Commons Attribution License, which permits use, distribution and reproduction in any medium, provided the original work is properly cited.

metal ion that fit with the coordination preferences of either Cu^{II} or Cu^{I} . For instance, in the case of the $A\beta$ peptide, both Cu^{II} and Cu^{I} bind to the N-terminal domain ($A\beta_{1-16}$)^[14-16] (see Figure 1). Cu^{II} is predominantly coordinated in a distorted square-pyramidal geometry via 3 nitrogen and 1 oxygen equatorial ligands and a weaker O axial ligand.^[17] The coordination of $\text{Cu}^{\text{II}}-A\beta$ is pH-dependent. In particular, two species co-exist at physiological pH 7.4 (notably, a major component I and a minor component II^[18,19]), with component I becoming the only present species at more acidic pH.^[19] Cu^{I} preferentially binds in a linear geometry with two nitrogen atoms^[9] from the imidazole rings of two His residues (see Figure 1). These two coordination modes represent the resting states, i.e. the most populated conformations coexisting in fast equilibrium with other less populated conformations.^[20]

Thus, the very different coordination sphere of the two resting states raises the question of how the redox cycling can occur. In fact, a quite important rearrangement of the peptide around the Cu ion is required upon Cu reduction/oxidation, which normally leads to a sluggish redox reaction and hence low ROS production.^[20,22]

In order to explain the relatively efficient ROS production by $\text{Cu}-A\beta$, it has been suggested that the latter is catalyzed by a low populated Cu-state, called an “in-between” state that can cycle between Cu^{I} and Cu^{II} redox states with little atomic rearrangement and hence produce efficiently ROS.^[22] In-between states attracted a lot of interest as only this state seems to be redox competent enough to efficiently generate ROS and hence is the state of choice as the target for suppressing ROS production by $\text{Cu}-A\beta$.

However, although experimental and theoretical evidence have suggested candidates for the “in-between” state^[21,23-25] (see Figure 1), a direct experimental evidence of its structure is lacking so far, mainly as a result of the challenging experimental characterization of such a low populated species (estimated to be 0.1 % of the total from electrochemical studies).^[22] A previous X-ray Absorption Spectroscopy (XAS) study has investigated the structure of

Cu -truncated $A\beta$ complexes under in situ electrochemically-induced reduction.^[26]

In this work, we aimed at trapping and characterizing possible intermediates in $\text{Cu}-A\beta_{1-16}$ redox cycling via XAS measurements at the Cu K-edge.

In order to ensure sample homogeneity, the soluble N-terminal $A\beta_{1-16}$ peptide fragment was used instead of the full-length $A\beta_{1-42}$. Indeed, since $A\beta_{1-16}$ very well reproduces the coordination of Cu^{II} and Cu^{I} to $A\beta_{1-42}$, $A\beta_{1-40}$ and $A\beta_{1-28}$, it is often used as a model for the longer peptide.^[15,27,28]

It is well known that, in the physical conditions of standard XAS experiments, which are typically performed at a temperature as low as 10 K, a progressive reduction of Cu^{II} to Cu^{I} is observed in the $\text{Cu}-A\beta_{1-42}$ peptide complex in vitro.^[29] However, the systematic study of the behavior of $\text{Cu}-A\beta$ complexes^[30] has shown that, despite the progressive reduction of Cu^{II} to Cu^{I} , at 10 K the spatial organization of the ligands did not change, yielding a Cu^{I} ion in a coordination sphere of the Cu^{II} resting state. In the present work, the samples were irradiated with a high X-ray dose at 10 K. To allow partial relaxation of the ligands around Cu, the temperature was raised up to 200 K with the aim of producing and trapping non-resting states, which were then structurally characterized by XAS. As detailed in the following, we were able to promote the formation of a complex different from both resting states and to characterize its structure.

XAS measurements at the Cu K-edge were performed at the BM30 beamline of the European Synchrotron Radiation Facility (ESRF—Grenoble, France).^[31] In order to identify possible intermediate species appearing during the $\text{Cu}^{\text{I}}-A\beta_{1-16}$ photoreduction process, the spectra of $\text{Cu}^{\text{I}}-A\beta_{1-16}$ and $\text{Cu}^{\text{II}}-A\beta_{1-16}$ resting states were first recorded. In order to avoid the co-presence of different Cu^{II} species, samples were prepared at pH 5.7, where only component I is known to be present.^[19] As detailed in the first two rows of Table 1, that contains the list of the collected spectra, the resting states were measured keeping the samples at the temperature of 10 K and averaging 5 scans, each one acquired in a different spot on the sample. In this way, the possible effects due to

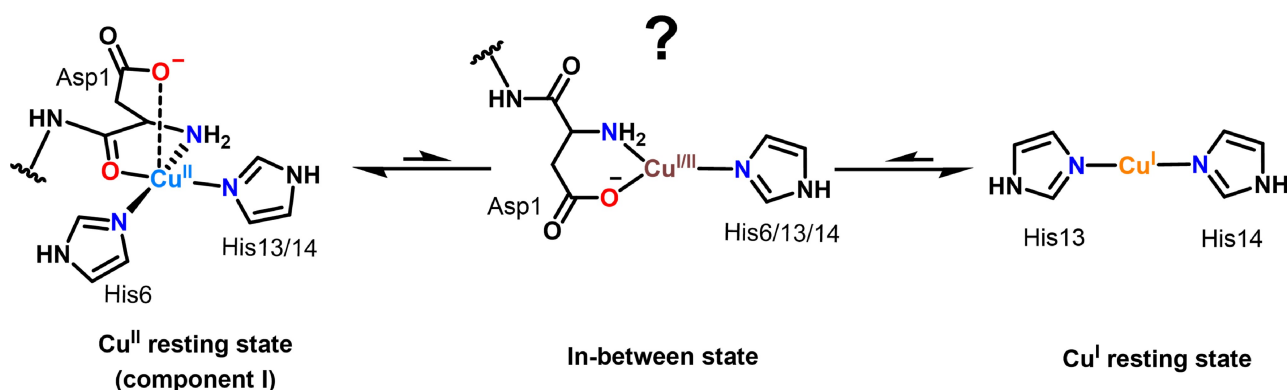


Figure 1. Structure of the most populated Cu^{II} and Cu^{I} resting states and proposed structure of the catalytic “in-between” state, which seems to involve the amino terminal nitrogen and side-chain carboxylate oxygen from Asp1 and an imidazole from either His 6, 13 or 14 (with no preference for any of the three His residues).^[21]

Table 1: List of the measured samples. In all the samples, except in the case of $\text{Cu}^{\text{I}}\text{-A}\beta_{1-16}$ in the first row, the initial Cu oxidation state is Cu^{II} . In the first column, we list the names of the samples. In the second column we give a short description of each sample and in the third column the temperature at which each spectrum was collected is indicated.

Sample name	Sample description	T [K]
$\text{Cu}^{\text{I}}\text{-A}\beta_{1-16}$	average over 5 spectra each acquired by hitting a new spot	10
$\text{Cu}^{\text{II}}\text{-A}\beta_{1-16}$	average over 5 spectra each acquired by hitting a new spot	10
S1 ₁₀	hitting a new spot on $\text{Cu}^{\text{II}}\text{-A}\beta$	10
S2 ₁₀	same spot as S1	10
S3 ₁₀	same spot as S1 ₁₀ and S2 ₁₀	10
S4 ₁₀	same spot as S1 ₁₀ , S2 ₁₀ and S3 ₁₀	10
S5 ₁₀	same spot as S1 ₁₀ , S2 ₁₀ , S3 ₁₀ and S4 ₁₀	10
S6 ₁₀₋₂₀₀₋₁₀	same spot as S1 ₁₀ , S2 ₁₀ , S3 ₁₀ , S4 ₁₀ and S5 ₁₀ after a temperature cycle	10→200→10
S1 ₂₀₀	new spot on $\text{Cu}^{\text{II}}\text{-A}\beta$ at high temperature	200
S2 ₂₀₀	same spot as S2 ₂₀₀	200
S3 ₂₀₀	same spot as S1 ₂₀₀ and S2 ₂₀₀	200

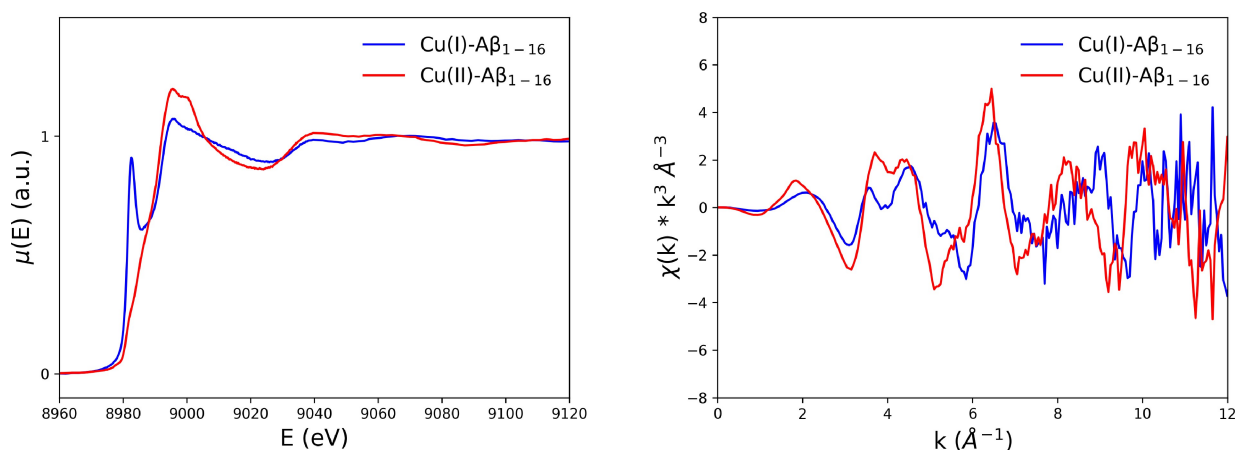


Figure 2. Comparison of the XAS spectra of $\text{Cu}^{\text{I}}\text{-A}\beta_{1-16}$ (blue lines) and $\text{Cu}^{\text{II}}\text{-A}\beta_{1-16}$ (red lines) complexes. Left panel, XANES. Right panel, EXAFS.

Table 2: $\text{Cu}^{\text{I}}\text{-A}\beta_{1-16}$ and $\text{Cu}^{\text{II}}\text{-A}\beta_{1-16}$ ligand distances, Fermi energy shift, E_{F} , and R-factor of the optimized EXAFS fits.

$\text{Cu}^{\text{I}}\text{-A}\beta_{1-16}$			$\text{Cu}^{\text{II}}\text{-A}\beta_{1-16}$		
Ligand	Distance [Å]	σ^2 [Å ²]	Ligand	Distance [Å]	σ^2 [Å ²]
2 N (His)	1.88 ± 0.01	0.003 ± 0.001	2 N (His)	1.97 ± 0.01	0.004 ± 0.001
			1 O	2.02 ± 0.01	0.004 ± 0.001
			1 N	1.94 ± 0.01	0.004 ± 0.001
$E_{\text{F}} = (-3.2 \pm 0.9)$ eV			$E_{\text{F}} = (2.8 \pm 0.7)$ eV		
R-factor = 32%			R-factor = 32%		
BVS = 0.9 ^[a]			BVS = 1.9		

[a] This value of BVS is obtained using the parameters from Ref. [14]. Using the latest 2020 IUCr Cu(I) parameters from <https://www.iucr.org/resources/data/datasets/bond-valence-parameters> one gets BVS = 0.7.

the interaction with the X-ray beam were minimized while the signal-to-noise ratio was improved.

As shown in Figure 2, $\text{Cu}^{\text{I}}\text{-A}\beta_{1-16}$ and $\text{Cu}^{\text{II}}\text{-A}\beta_{1-16}$ samples exhibit visibly different XAS spectra, thus confirming, in agreement with spectra from the literature,^[14,20] that the $\text{Cu}\text{-A}\beta_{1-16}$ coordination mode is strongly dependent on the Cu oxidation state.

The XANES (X-ray Absorption Near Edge Spectroscopy) region of $\text{Cu}^{\text{I}}\text{-A}\beta_{1-16}$ (left panel of Figure 2), shows a

peak, located in the pre-edge region at about 8982.6 eV, that is known^[14,29,32,33] to be the fingerprint of Cu^{I} presence.

Quantitative structural information can be obtained from a fit of the EXAFS (Extended X-ray Absorption Fine Structure) region of the spectrum. We report in Table 2 the values of the best-fit parameters, including the quality factor R,¹ that provides a quantitative measure of the goodness of the fit. The best fit of the $\text{Cu}^{\text{I}}\text{-A}\beta_{1-16}$ complex EXAFS

¹ The quality factor R is defined as $R\text{-factor} = \frac{\sum_i |x^{\text{exp}}(k_i) - x(k_i)^{\text{fit}}|}{\sum_i |x^{\text{exp}}(k_i)|}$.

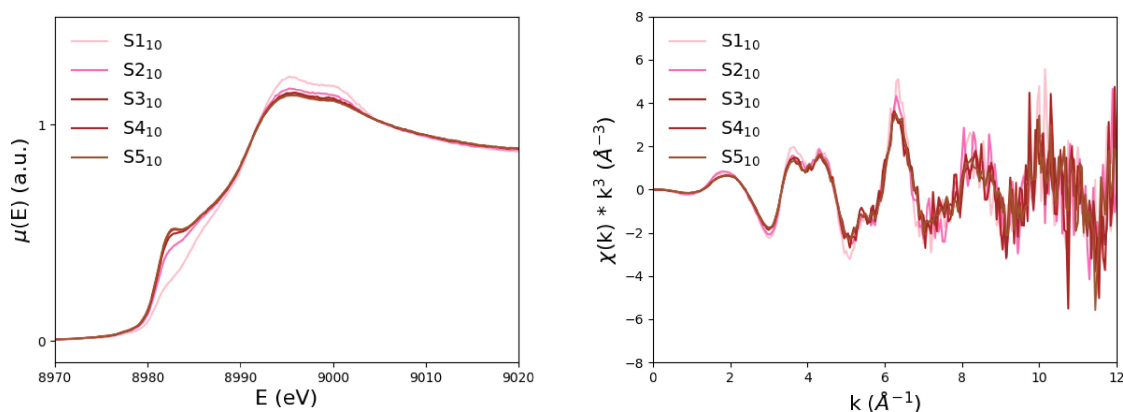


Figure 3. The five consecutive scans of $\text{Cu}^{\text{II}}\text{-A}\beta_{1-16}$ complexes in the XANES (left panel) and EXAFS (right panel) regions at increasing X-ray dose.

spectrum is obtained by assuming that only two ligands, namely two nitrogen atoms from two imidazole rings of two His residues, are coordinated to Cu^{I} .

The fit to the $\text{Cu}^{\text{II}}\text{-A}\beta_{1-16}$ EXAFS data shows instead that the Cu^{II} coordination mode involves four ligands, namely two nitrogen atoms from two His residues plus one nitrogen and one oxygen from the Asp residue. Comparisons between experimental data and best fits and the corresponding Fourier Transforms (FTs) of both spectra are provided in the Supporting Information (Figure S1).

XANES calculations were then performed using the FDMNES code^[34,35] starting from the best-fit EXAFS models. Figure S3 shows the comparison between the XANES simulations and the corresponding experimental data. The qualitative agreement between simulated and experimental data is quite good, thus corroborating the results of the EXAFS analysis. Sketches of the structures coming from the EXAFS fits and used for the XANES calculations are given in Figure S3.

Finally, the Bond Valence Sum (BVS) was computed for both best-fit models and reported in the last row of Table 2. The BVS values are in quite good agreement with the corresponding Cu oxidation states.²

In order to follow the possible evolution of the spectrum induced by X-ray irradiation, we further collected five spectra, one after the other, by letting the beam hit the same point of the sample and keeping the sample at 10 K. Taking into account the photon flux, the beam size, the sample thickness (2 mm) transmission and the exposure time (each scan lasted about 40 minutes), the dose absorbed by the sample in a single scan is estimated to be around 9×10^6 Gy.

In Figure 3 we show the “time evolution” of the XANES (left panel) and EXAFS (right panel) data by plotting one on top of the other the five consecutively collected spectra. In Figure S4 the corresponding FTs are also shown. The increasing intensity of the shoulder at 8982.6 eV is a clear

confirmation of the fact that X-ray radiation induces the $\text{Cu}^{\text{II}} \rightarrow \text{Cu}^{\text{I}}$ reduction process.^[30]

On the other hand, looking at the EXAFS region (Figure 3, right panel) we see that the spectral evolution with beam exposure time is marginal, as already noticed previously.^[30] In other words, at such a low temperature, there are no major structural rearrangements associated with the modification of the Cu oxidation state. Looking at the comparison of $\text{Cu}^{\text{I}}\text{-A}\beta_{1-16}$ with S1₁₀ and S5₁₀, shown in Figure 4 (the FTs are shown in Figure S5), it is clear that, even in the presence of radiation-induced Cu reduction, the Cu coordination mode is unable to turn into that of the $\text{Cu}^{\text{I}}\text{-A}\beta_{1-16}$ resting structure. A quantitative estimation of similarities among these spectra is provided in the Supporting Information.

After collecting the five XAS spectra with the beam hitting always the same sample spot, the X-ray beam was switched off and the sample temperature was increased to 200 K in order to accelerate a possible, but not total, structural relaxation, associated to the presence of reduced Cu, while still keeping the sample in a frozen, solid state. Once the temperature reached 200 K, the sample was cooled back to 10 K. The whole heating and cooling cycle took about 100 minutes, after which a new XAS spectrum, termed S6₁₀₋₂₀₀₋₁₀ in Table 1, was collected in the previously exposed sample position.

Again in Figure 4 we compare the spectrum of the S6₁₀₋₂₀₀₋₁₀ sample with that of the last (S5₁₀) and the first (S1₁₀) spectrum of the series previously collected as well as with the $\text{Cu}^{\text{I}}\text{-A}\beta_{1-16}$ spectrum. The difference among the spectra of S1₁₀ (which is nothing but the $\text{Cu}^{\text{II}}\text{-A}\beta_{1-16}$ resting state), S6₁₀₋₂₀₀₋₁₀ and $\text{Cu}^{\text{I}}\text{-A}\beta_{1-16}$ must be attributed to the fact that the state obtained upon heating/cooling is different from the two resting states. S6₁₀₋₂₀₀₋₁₀ is also different from S5₁₀, thus suggesting that the increase in temperature allowed the sample to undergo a structural relaxation that did not take place at 10 K.

Moreover, in the S6₁₀₋₂₀₀₋₁₀ spectrum the intensity of the shoulder that indicates the presence of Cu^{I} is significantly lower than in the S5₁₀ case, a feature which might be indicative of a partial re-oxidation of Cu^{I} to Cu^{II} or of a modification in coordination geometry.^[32] In addition, the

²BVS provides a simple way to estimate the oxidation state of an atom in a given structure. Its value, which depends on the type, number, and distances of ligands, should agree with the nominal value of the oxidation state.^[36]

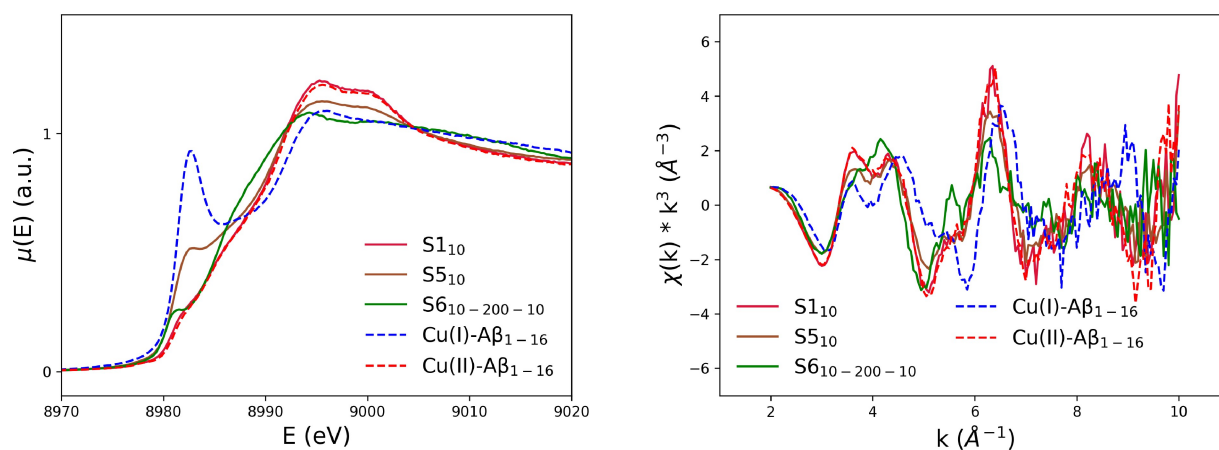


Figure 4. Comparison among the spectra of the $S6_{10-200-10}$, $S1_{10}$, $S5_{10}$, $Cu^I-A\beta_{1-16}$ and $Cu^{II}-A\beta_{1-16}$ in the XANES (left panel) and EXAFS (right panel) regions.

pre-edge peak appears to be shifted toward lower energy in $S6_{10-200-10}$ with respect to $S5_{10}$, i.e. 8981.2 eV vs. 8982.6 eV. Qualitatively, this difference in energy may be associated to a different Cu coordination geometry occurring in the two samples. This interpretation reinforces the idea of having different structural atomic arrangements around the metal in $S6_{10-200-10}$ and $S5_{10}$, and not simply a difference in the Cu oxidation state.

This interesting hypothesis is further supported by the fact that the spectrum of $S6_{10-200-10}$ can not be well reproduced as a linear combination of $Cu^{II}-A\beta_{1-16}$ and $Cu^I-A\beta_{1-16}$ spectra (see Figure S5 in Supporting Information). This allows us to conclude that $S6_{10-200-10}$ does not represent a mere combination of the two resting states and therefore that a relaxation towards a coordination mode different from both resting states takes place when the sample is brought to 200 K.

In order to better characterize the effect of temperature on the spectra, three consecutive scans were acquired at 200 K with the beam hitting a fixed spot. The spectral evolution is faster at 200 K than at 10 K and the Cu^I peak, located in the pre-edgeregion, appears already in the first

scan, $S1_{200}$. Since the energy corresponding to the Cu^I peak is measured during the scan after about 10 minutes of exposure, we argue that, at 200 K, the oxidation state switch occurs on a timescale shorter than the acquisition time of a single XANES spectrum. This is confirmed by the fact that $S1_{200}$, $S2_{200}$ and $S3_{200}$ only exhibit marginal differences (see the comparison among $S1_{200}$, $S2_{200}$ and $S3_{200}$ spectra in Figure S7 in Supporting Information). However, the comparison between $S3_{200}$ and $Cu^I-A\beta$ (Figure 5) clearly shows that not even the exposure of the Cu^{II} sample to X-rays for as long as 2 hours (which is the time necessary to acquire 3 consecutive scans) at 200 K lead to the same spectrum as the Cu^I resting state.

Based on the fact that, as we have argued, the “relaxed” coordination mode of $S6_{10-200-10}$ is neither that of $Cu^I-A\beta_{1-16}$ nor that of $Cu^{II}-A\beta_{1-16}$, we tried fitting the EXAFS data taking as a starting configuration the putative “in-between” $Cu^I/Cu^{II} A\beta_{1-16}$ model suggested in Ref. [25], which is in agreement with the experimental findings of Ref. [21].

More in detail, we started from a slightly modified version of model 14 from Ref. [25], in which the O_2 molecule present in the structure was substituted by a water molecule.

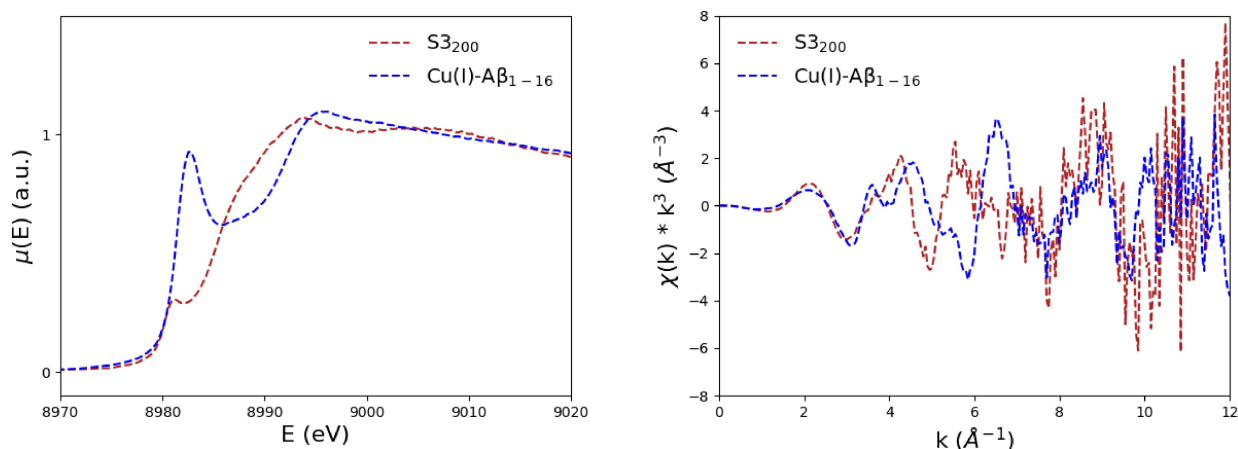


Figure 5. Comparison between the $Cu^I-A\beta_{1-16}$ and $S3_{200}$ XANES (left panel) and EXAFS (right panel) spectra.

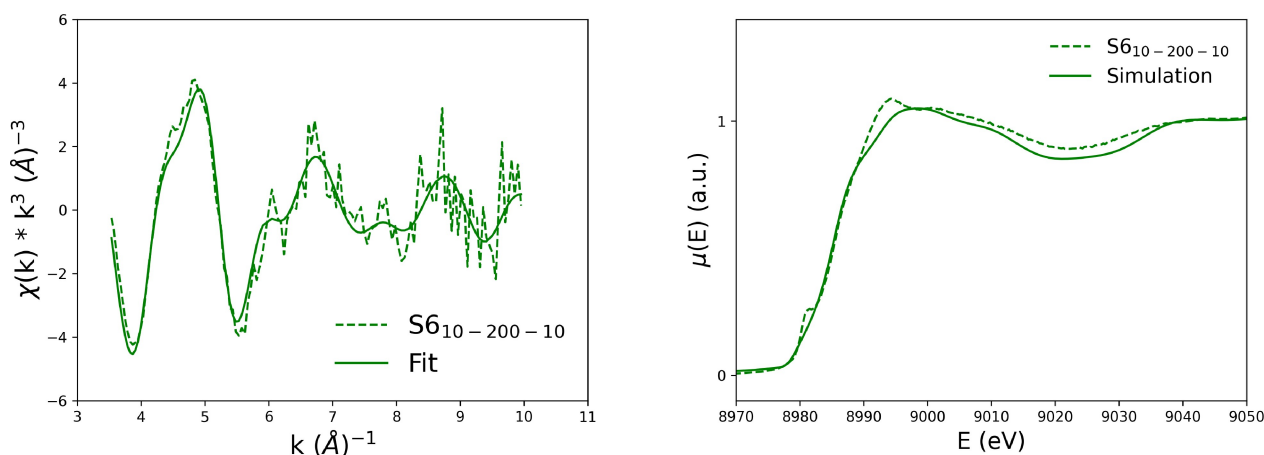


Figure 6. Left panel: experimental (broken line) and fitted (solid line) EXAFS data of sample $S6_{10-200-10}$. Right panel: XANES calculations performed starting from the EXAFS best-fit model (solid line) superimposed to the XANES experimental data (broken line).

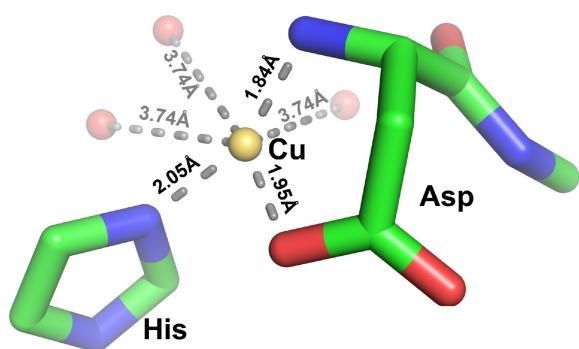


Figure 7. A sketch of the best-fit structure of the Cu coordination site in the $S6_{10-200-10}$ sample. Cu is in yellow, N in blue, C in green and O in red. The three O atoms belonging to water molecules are drawn in a fainter red, since they do not belong to the first coordination shell.

Table 3: $S6_{10-200-10}$ ligand distances and Fermi energy shift at the end of the EXAFS fit. We also report the values of the R-factor and of the BVS parameter.

Ligand	Distance [Å]	σ^2 [Å ²]
1 N (His)	2.05 ± 0.02	0.003 ± 0.001
1 N (Asp)	1.84 ± 0.02	0.003 ± 0.001
1 O (Asp)	1.95 ± 0.02	0.003 ± 0.001
3 O (Water)	3.74 ± 0.03	0.005 ± 0.001

$E_F = (-7 \pm 1)$ eV

R-factor = 34 %

BVS = 1.5^[a]

[a] This value of BVS is obtained using the Cu(II) parameters from Ref. [14]. Using the latest 2020 IUCr Cu(I) parameters from <https://www.iucr.org/resources/data/datasets/bond-valence-parameters> one gets BVS = 1.0.

This starting model was then relaxed by minimizing its total energy. We used the hybrid exchange-correlation functional suitable to Cu complexes already employed in Ref. [25] (and references therein). In the first coordination shell of the model there are an imidazole ring belonging to a His residue, the N-terminal amine nitrogen, and an oxygen atom

belonging to the Asp1 side chain. Three water molecules, located within 5 Å from the Cu ion, but not belonging to the first coordination shell, are also included.

The best-fit spectrum obtained starting from the above configuration is in quite good agreement within the signal-to-noise ratio with the experimental EXAFS data (see Figure 6, left panel; the corresponding FTs are shown in Figure S8), thus suggesting that, after X-ray exposure, by heating and cooling the sample, Cu actually reaches an “intermediate” coordination mode like the one depicted in Figure 7. The best-fit parameters are reported in Table 3. The XANES spectrum calculated from the best-fit EXAFS model is remarkably well superimposable to the experimental data (Figure 6, right panel), with differences (in the pre-edge feature and in the so-called white-line, i.e. the main peak after the absorption edge) likely due to a not perfect description of the geometry around the absorbing atom as well as to a rigid description of this geometry that does not take into account both angular and linear disorders. It is worth noticing that the BVS value associated to the best-fit structure lies halfway between 1 and 2, supporting the idea that the combination of distances and coordination number is neither what is expected for a pure Cu^I nor a pure Cu^{II} oxidation state.

Since our experiment started from the Cu^{II} resting state, to reach the conjectured in-between state the following rearrangement would have to occur. One of the two Cu-His bonds should be broken (previous experiments showed no preference for any of the three His)^[21] with the His moving away at least to a non-bonding distance to Cu^I. In addition, Asp1 carbonyl should also detach from Cu, while a bond is formed with its nearby (and possibly already axially bound) carboxylate. This structural rearrangement does not involve major changes in the peptide main chain and therefore it is likely compatible with structural changes observed in proteins at cryogenic temperatures.^[37,38]

For the sake of completeness, also a significantly different putative “in-between” structure (model 9 in the nomenclature of Ref. [25]), in which two imidazole rings and the amino group of Asp1 are bound to Cu, was considered. The

agreement between a fit starting from this model and the experimental data obtained is both qualitatively and quantitatively (R-factor=41 %) worse than the one described in Table 3 (R-factor=34 %), suggesting that, although our data cannot rule out the coexistence of different coordination structures, a three-coordinated model with one His residue and a bi-dentate Asp is the best “in-between” coordination mode candidate.

In this work we have exploited a well-known side-effect of exposure to high-intensity X-ray beams on Cu complexes, that is Cu reduction, to try to access a possible “in-between” Cu^I-Aβ₁₋₁₆ and Cu^{II}-Aβ₁₋₁₆ coordination mode.

We have used the X-ray beam to pump Cu^{II}-Aβ₁₋₁₆ complexes in a non-resting state by promoting Cu^{II} reduction to Cu^I, keeping the system at a temperature of 10 K. The sample temperature was then raised to 200 K to allow possible structural modifications associated with oxidation state changes. Finally, the XAS spectrum of the system was acquired after cooling down the sample at 10 K. We observe that the measured spectrum is different from the spectra of both resting states. A quantitative EXAFS analysis shows that it is compatible with a possible “in-between” structure suggested by previous experiments and numerical simulations^[25] and characterized by the presence of a single imidazole ring and a bi-dentate Asp residue in the Cu coordination site. The EXAFS results are corroborated by an ab initio XANES simulation performed starting from the EXAFS best-fit structure, which leads to results in good agreement with the experimental data.

The experimental approach used in this work provides the first direct evidence and structural characterization of an intermediate of Cu^{II}-Aβ₁₋₁₆ reduction, supporting the existence and identity of a previously postulated redox-active “in-between” state. Moreover, we showed that the X-ray-induced photo-reduction, which is normally an undesired side effect of overexposure to X-ray beams, can also be tamed to pump metal-peptide complexes into not-resting states that could be relevant for their catalytic activity. Hence, our work paves the way for the exploration of further redox intermediates formed by biological and non-biological metal complexes.

Note added in proof after first online publication of the Accepted Article: the final version of record of this Communication contains an additional reference (Ref. [26]) reporting an XAS study of Cu-truncated Aβ complexes under electrochemically-induced reduction that was missed during manuscript preparation. Also, two footnotes with the results obtained calculating the BVS applying the latest, 2020 IUCr Cu(I) parameters, since some less updated values coming from Ref. [14] were used in the Accepted Article, were added.

Acknowledgements

We acknowledge the European Synchrotron Radiation Facility (ESRF) for access to beam time and infrastructure (proposal LS-2968). Numerical calculations have been made possible owing to a CINECA-INFN agreement, providing

access to resources on MARCONI at CINECA. This work was partially supported by the BIOPHYS initiative (INFN, Italy). E.F. and M.O. acknowledge financial support from the French National Research Agency (Programme d'Investissement d'Avenir under contract 17-EURE-0016) and from the IDEX program (University of Strasbourg), respectively. S.M. and F.S. acknowledge financial support from the “PANDA” project, University of Rome Tor Vergata.

Conflict of Interest

The authors declare no conflict of interest.

Data Availability Statement

The data that support the findings of this study are available from the corresponding author upon reasonable request.

Keywords: Amyloid β · Copper Oxidation State · EXAFS · X-Ray Absorption Spectroscopy · in-Between State

- [1] B. Kim, T. Nevitt, D. J. Thiele, *Nat. Chem. Biol.* **2008**, *4*, 176–185.
- [2] S. Lutsenko, *J. Cell Sci.* **2021**, *134*, jcs240523.
- [3] D. Brancaccio, A. Gallo, M. Piccioli, E. Novellino, S. Ciofi-Baffoni, L. Banci, *J. Am. Chem. Soc.* **2017**, *139*, 719–730.
- [4] L. Macomber, J. A. Imlay, *Proc. Natl. Acad. Sci. USA* **2009**, *106*, 8344–8349.
- [5] P. Tsvetkov, S. Coy, B. Petrova, M. Dreishpoon, A. Verma, M. Abdusamad, J. Rossen, L. Joesch-Cohen, R. Humaidi, R. D. Spangler, et al., *Science* **2022**, *375*, 1254–1261.
- [6] L. Zuily, N. Lahrach, R. Fassler, O. Genest, P. Faller, O. Seneque, Y. Denis, M.-P. Castanie-Cornet, P. Genevaux, U. Jakob, et al., *mBio* **2022**, *13*, e03251-21.
- [7] S. Morante, *Curr. Alzheimer Res.* **2008**, *5*, 508–524.
- [8] K. J. Barnham, A. L. Bush, *Chem. Soc. Rev.* **2014**, *43*, 6727–6749.
- [9] E. Atrián-Blasco, P. Gonzalez, A. Santoro, B. Alies, P. Faller, C. Hureau, *Coord. Chem. Rev.* **2018**, *371*, 38–55.
- [10] J.-H. Ye, T. Ju, H. Huang, L.-L. Liao, D.-G. Yu, *Acc. Chem. Res.* **2021**, *54*, 2518–2531.
- [11] K. Acevedo, S. Masaldan, C. M. Opazo, A. I. Bush, *J. Biol. Inorg. Chem.* **2019**, *24*, 1141–1157.
- [12] P. Faller, C. Hureau, G. La Penna, *Acc. Chem. Res.* **2014**, *47*, 2252–2259.
- [13] G. La Penna, S. Morante, *Aggregates Sealed by Ions, in Computer Simulations of Aggregation of Proteins and Peptides*, Springer, Cham, **2022**, pp. 309–341.
- [14] J. Shearer, V. A. Szalai, *J. Am. Chem. Soc.* **2008**, *130*, 17826–17835.
- [15] V. Minicozzi, F. Stellato, M. Comai, M. Dalla Serra, C. Potrich, W. Meyer-Klaucke, S. Morante, *J. Biol. Chem.* **2008**, *283*, 10784–10792.
- [16] E. De Santis, V. Minicozzi, O. Proux, G. Rossi, K. I Silva, M. J. Lawless, F. Stellato, S. Saxena, S. Morante, *J. Phys. Chem. B* **2015**, *119*, 15813–15820.
- [17] P. Dorlet, S. Gambarelli, P. Faller, C. Hureau, *Angew. Chem. Int. Ed.* **2009**, *48*, 9273–9276.
- [18] C. D. Syme, R. C. Nadal, S. E. J. Rigby, J. H. Viles, *J. Biol. Chem.* **2004**, *279*, 18169–18177.

- [19] B. Alies, H. Eury, C. Bijani, L. Rechinat, P. Faller, C. Hureau, *Inorg. Chem.* **2011**, *50*, 11192–11201.
- [20] C. Hureau, V. Balland, Y. Coppel, P. L. Solari, E. Fonda, P. Faller, *J. Biol. Inorg. Chem.* **2009**, *14*, 995–1000.
- [21] C. Cheignon, M. Jones, E. Atrián-Hlasco, I. Kieffer, P. Faller, F. Collin, C. Hureau, *Chem. Sci.* **2017**, *8*, 5107–5118.
- [22] V. Balland, C. Hureau, J.-M. Savéant, *Proc. Natl. Acad. Sci. USA* **2010**, *107*, 17113–17118.
- [23] T. Prosdocimi, L. De Gioia, G. Zampella, L. Bertini, *J. Biol. Inorg. Chem.* **2016**, *21*, 197–212.
- [24] F. Arrigoni, T. Prosdocimi, L. Mollica, L. De Gioia, G. Zampella, L. Bertini, *Metallomics* **2018**, *10*, 1618–1630.
- [25] A. Mirats, J. Alli-Torres, L. Rodríguez-Santiago, M. Sodupe, G. La Penna, *Phys. Chem. Chem. Phys.* **2015**, *17*, 27270–27274.
- [26] V. A. Streltsov, R. S. K. Ekanayake, S. C. Drew, C. T. Chantler, S. B. Best, *Inorg. Chem.* **2018**, *57*, 11422–11435.
- [27] A. Abelein, S. Ciofi-Baffoni, C. Mörman, R. Kumar, A. Giachetti, M. Piccioli, H. Biverstäl, *JACS Au* **2022**, *2*, 2571–2584.
- [28] W. A. Gunderson, J. Hernández-Guzmán, J. W. Karr, L. Sun, V. A. Szalai, K. Warncke, *J. Am. Chem. Soc.* **2012**, *134*, 18330–18337.
- [29] K. L. Summers, K. M. Schilling, G. Roseman, K. A. Markham, N. V. Dolgova, T. Kroll, D. Sokaras, G. L. Millhauser, I. J. Pickering, G. N. George, *Inorg. Chem.* **2019**, *58*, 6294–6311.
- [30] F. Stellato, R. Chiaraluce, V. Consalvi, E. De Santis, G. La Penna, O. Proux, G. Rossi, S. Morante, *Metallomics* **2019**, *11*, 1401–1410.
- [31] O. Proux, X. Biquard, E. Lahera, J.-J. Menthonnex, A. Prat, O. Ulrich, Y. Soldo, P. Trévisson, G. Kapoujyan, G. Perroux, et al., *Phys. Scr.* **2005**, *2005*, 970.
- [32] L. S. Kau, D. J. Spira-Solomon, J. E. Penner-Hahn, K. O. Hodgson, E. I Solomon, *J. Am. Chem. Soc.* **1987**, *109*, 6433–6442.
- [33] C. Lamberti, S. Bordiga, F. Bonino, C. Prestipino, G. Berlier, L. Capello, F. D'Acapito, F. L. i Xamena, A. Zecchina, *Phys. Chem. Chem. Phys.* **2003**, *5*, 4502–4509.
- [34] O. Bunău, Y. Joly, *J. Phys. Condens. Matter* **2009**, *21*, 345501.
- [35] S. A. Guda, A. A. Guda, M. A. Soldatov, K. A. Lomachenko, A. L. Bugaev, C. Lamberti, W. Gawelda, C. Bressler, G. Smolentsev, A. V. Soldatov, et al., *J. Chem. Theory Comput.* **2015**, *11*, 4512–4521.
- [36] L. Brown, *Struct. Bonding Crystals* **1981**, *2*, 1–30.
- [37] A. Arcovito, T. Moschetti, P. D'Angelo, G. Mancini, B. Vallone, M. Brunori, S. Della Longa, *Arch. Biochem. Biophys.* **2008**, *475*, 7–13.
- [38] A. Regis Faro, P. Carpentier, G. Jonasson, G. Pompidor, D. Arcizet, L. Demachy, D. Bourgeois, *J. Am. Chem. Soc.* **2011**, *133*, 16362–16365.

Manuscript received: December 2, 2022

Accepted manuscript online: March 3, 2023

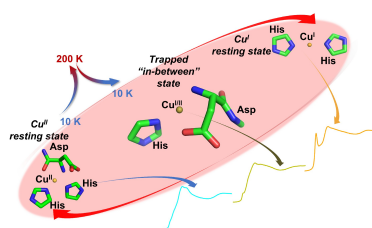
Version of record online: ■■■, ■■■

Communications

Amyloid-beta

E. Falcone, G. Nobili, M. Okafor, O. Proux,
G. Rossi, S. Morante, P. Faller,*
F. Stellato* [e202217791](#)

Chasing the Elusive “In-Between” State of the Copper-Amyloid β Complex by X-ray Absorption through Partial Thermal Relaxation after Photoreduction



The combination of X-ray induced photoreduction and thermal relaxation unravels the structure of an intermediate of the Cu^{II}/Cu^I A β ₁₋₁₆ redox cycling. The X-ray beam promotes Cu^{II} reduction to Cu^I at 10 K, then the sample undergoes partial structural relaxation at 200 K and a spectrum measured at 10 K is compatible with a possible “in-between” structure featuring an imidazole ring and a bi-dentate Asp residue in the Cu coordination site.